0026-895X/11/7902-229–240$20.00
MOLECULAR PHARMACOLOGY
Copyright © 2011 The American Society for Pharmacology and Experimental Therapeutics
Mol Pharmacol 79:229–240, 2011

Vol. 79, No. 2
69013/3658986
Printed in U.S.A.

MOL PHARM

Multidrug Resistance-Related Protein 1 (MRP1) Function and Localization Depend on Cortical Actin

Ina Hummel, Karin Klappe, Cigdem Ercan, and Jan Willem Kok

Department of Cell Biology, Section Membrane Cell Biology, University Medical Center Groningen, University of Groningen, Groningen, the Netherlands

Received September 21, 2010; accepted November 1, 2010

ABSTRACT

MRP1 (ABCC1) is known to be localized in lipid rafts. Here we show in two different cell lines that localization of Mrp1/MRP1 (Abcc1/ABCC1) in lipid rafts and its function as an efflux pump are dependent on cortical actin. Latrunculin B disrupts both cortical actin and actin stress fibers. This results in partial loss of actin and Mrp1/MRP1 (Abcc1/ABCC1) from detergent-free lipid raft fractions, partial internalization of Mrp1/MRP1 (Abcc1/ABCC1), and reduction of Mrp1/MRP1 (Abcc1/ABCC1)-mediated efflux. Pretreatment with nocodazole prevents latrunculin B-induced loss of cortical actin and all effects of latrunculin B on Mrp1 (Abcc1) localization and activity. However, pretreatment with tyrphostin A23 does not prevent latrunculin B-induced loss of cortical actin, lipid raft association, and efflux activity, but it does prevent latrunculin B-induced internalization of Mrp1 (Abcc1). Cytochalasin D disrupts actin stress fibers but not cortical actin and this inhibitor much less affects Mrp1/MRP1 (Abcc1/ABCC1) localization in lipid rafts, internalization, and efflux activity. In conclusion, cortical actin disruption results in reduced Mrp1/MRP1 (Abcc1/ABCC1) activity concomitant with a partial shift of Mrp1/MRP1 (Abcc1/ABCC1) out of lipid raft fractions and partial internalization of the ABC transporter. The results suggest that reduced Mrp1 (Abcc1) function is correlated to the loss of lipid raft association but not internalization of Mrp1 (Abcc1).

Introduction

One of the best characterized multidrug resistance (MDR) mechanisms is the overexpression of ATP-binding cassette (ABC) transporter proteins, which prevent intracellular drug accumulation. Among these proteins, P-glycoprotein (PGP/Pgp or ABCB1/ Abcb1) and multidrug resistance-related protein 1 (Mrp1/MRP1 or Abcc1/ABCC1) are the most widely studied. Both ABC transporters are known to depend on their direct lipid environment in model membranes for optimal functioning (Sinicrope et al., 1992; Dudeja et al., 1995). Pgp (Abcb1) was found to have a higher affinity for its substrates when the surrounding lipids are in the liquid-ordered phase rather than in the liquid-disordered phase (Romsicki and Sharom, 1999). The liquid-ordered phase occurs when lipids have a high degree of saturation, like sphingolipids, which enables them to pack tightly. This is a putative characteristic of membrane microdomains or lipid rafts (including caveolae) in living cells as well (Schroeder et al., 1994; Brown and London, 2000).

Lavie et al. (1998) have shown for the first time the association of an ABC transporter with a membrane domain. They found that a substantial fraction of PGP (ABCB1) in PGP (ABCB1)-overexpressing cells was located in Triton X-100-based detergent-resistant membranes containing caveolin 1 (Cav-1). On the other hand, it was shown that PGP (ABCB1) and MRP1 (ABCC1) were not associated with caveolae in two human MDR tumor cell lines. Both MRP1 (ABCC1) and PGP (ABCB1) were found to be enriched in membrane domains defined by their insolubility in the nonionic detergent Lubrol. In 2780AD cells, PGP (ABCB1) was located in noncaveolar detergent-resistant membranes, because these cells did not express Cav-1 and hence lack caveolae. HT29^{col} cells did express Cav-1, but MRP1 (ABCC1) and Cav-1 did not colocalize and were not coimmunoprecipitated (Hinrichs et al., 2004). Another study also reported dissociation of Pgp (Abcb1) from caveolae in an MDR Chinese hamster ovary cell line and postulated that Pgp (Abcb1) resides in an intermediate-density membrane microdomain, which is

Article, publication date, and citation information can be found at http://molpharm.aspetjournals.org.
doi:10.1124/mol.110.069013.

ABBREVIATIONS: MDR, multidrug resistance; ABC, ATP-binding cassette; Cav-1, caveolin-1; CFDA, 5-carboxyfluorescein diacetate; Mrp1, murine multidrug resistance-related protein 1; MRP1, human multidrug resistance-related protein 1; PGP/Pgp, P-glycoprotein; ERM, ezrin, radixin, and moesin; HBSS, Hanks' balanced salt solution; FCS, fetal calf serum; PNS, postnuclear supernatant; PBS, phosphate-buffered saline; RT, room temperature; RT-PCR, reverse transcriptase-polymerase chain reaction; bp, base pair(s); DCI, direct competitive inhibitor; MK571, (*E*)-3-[[[3-[2-(7-chloro-2-quinolinyl)ethenyl]phenyl]-[[3-dimethylamino)-3-oxopropyl]thio]methyl]thio]-propanoic acid.

MOLECULAR PHARMACOLOGY
aspet
Downloaded from molpharm.aspetjournals.org by guest on December 1, 2012

MOL PHARM

MOLECULAR PHARMACOLOGY

distinct from both caveolar domains and classic lipid rafts and which is defined by insolubility in Brij-96 (decaethoxy oleoyl ether) (Radeva et al., 2005).

Formation and maintenance of lipid rafts seem to depend on specific lipids, namely sphingolipids and cholesterol. Lipid rafts are often considered to be highly dynamic entities, which may arise and dissolve continuously. On the other hand, the actin cytoskeleton seems to have the potential to stabilize them, at least temporarily. In fact, cortical actin may confer dynamic properties on lipid rafts, stabilizing them as separate domains upon actin binding, whereas the lipid rafts are able to move laterally and coalesce when disconnected from the actin cytoskeleton (Chichili and Rodgers, 2007). It is noteworthy that PGP (ABCB1) has been shown to be partially linked to the actin cytoskeleton (Bacso et al., 2004). Moreover, PGP (ABCB1)-actin association through ezrin, radixin, and moesin (ERM family proteins) has been shown in a MDR variant of a human T-lymphoblastoma cell line CEM-VBL100. Down-regulation of all three ERM proteins resulted in the loss of PGP (ABCB1)-actin association, PGP (ABCB1) redistribution, and concomitant sensitization to vinblastine, which accumulated because of the reduction of PGP (ABCB1)-mediated drug efflux. These data indicate that the ERM protein-mediated link between PGP (ABCB1) and F-actin is functional in MDR (Luciani et al., 2002). Another example of ABC transporter-actin associations mediated by ERM proteins is the direct association of radixin with the carboxyl-terminal cytoplasmic domain of human MRP2 (ABCC2), which was discovered in Rdx(−/−) mice (Kikuchi et al., 2002). Radixin deficiency in these mice results in the loss of MRP2 (ABCC2) from bile canalicular membranes, which leads to conjugated hyperbilirubinemia, a phenotype very similar to that of Dubin-Johnson syndrome characterized by mutations in *MRP2/ABCC2*, encoding MRP2. Thus, the ERM protein radixin in liver cells is essential for the correct localization of MRP2 (ABCC2) and its function in conjugated bilirubin secretion. However, for the family member Mrp1/MRP1 (Abcc1/ABCC1), no (direct or indirect) link to the actin cytoskeleton is known.

In this study, we investigated the affect of disruption of the actin cytoskeleton on the localization of Mrp1/MRP1 (Abcc1/ABCC1) and its efflux function. We studied subcellular localization of Mrp1/MRP1 (Abcc1/ABCC1) by confocal microscopy and its submembrane localization by nondetergent lipid raft analysis. Mrp1/MRP1 (Abcc1/ABCC1) function was determined by an efflux assay. We conclude that cortical actin stabilizes Mrp1/MRP1 (Abcc1/ABCC1) efflux activity and its localization in lipid rafts on the cell surface. Studies using tyrphostin A23 to inhibit Mrp1 (Abcc1) internalization suggest that reduction of Mrp1 (Abcc1) function is correlated to the loss of lipid raft association, but not internalization, of the ABC transporter.

Materials and Methods

Materials. (*E*)-3-[[[3-[2-(7-Chloro-2-quinolinyl)ethenyl]phenyl]-[[3-dimethylamino)-3-oxopropyl]thio]methyl]thio]-propanoic acid (MK571) was a gift from Dr. A.W. Ford-Hutchinson (Merck-Frosst, Inc., Kirkland, Canada). The monoclonal anti-giantin antibody was a gift from Dr. Hauri (Department of Pharmacology, University of Basel, Basel, Switzerland). Costar cell culture plastic was from Corning (Lowell, MA). RNeasy Mini Kit was obtained from QIAGEN (Valencia, CA). Cell culture media, Hanks' balanced salt solution (HBSS), antibiotics, L-glutamine, sodium pyruvate, trypsin, Platinum Blue PCR SuperMix, primers and all reagents for reverse transcription were from Invitrogen (Paisley, UK). Fetal calf serum (FCS) was from Bodinco (Alkmaar, The Netherlands). Latrunculin B, cytochalasin D, nocodazole, 5-carboxyfluorescein diacetate, rhodamine 123, TRI reagent, and the monoclonal anti-β-actin antibody were obtained from Sigma-Aldrich (St. Louis, MO). Cyclosporin A was from Alexis (Carlsbad, CA). Jasplakinolide was from Calbiochem (La Jolla, CA). Tyrphostin A23 was obtained from Santa Cruz Biotechnology Inc. (Santa Cruz, CA). Phalloidin Alexa Fluors 488 and 633 and all Alexa Fluor-conjugated secondary antibodies were obtained from Molecular Probes (Carlsbad, CA). OptiPrep was from Axis-Shield PoC AS (Dundee, Scotland). C12-fatty acid homologs of ceramide, sphingomyelin, glucosylceramide, and lactosylceramide were from Avanti Polar Lipids (Alabaster, AL). The rat monoclonal anti-MRP1 (ABCC1) (MRPr1) antibody was obtained from Signet Laboratories (Dedham, MA). The polyclonal anti-Cav-1 antibody was from Transduction Laboratories (Lexington, KY). The monoclonal anti-transferrin receptor antibody was from Zymed Laboratories (South San Francisco, CA).

Cell Culture and Incubation Conditions. The murine neuroblastoma cell line Neuro-2a was purchased from the American Type Culture Collection (Manassas, VA). These cells were grown as adherent monolayer cultures in Dulbecco's modified Eagle's medium supplemented with 10% FCS, 100 U/ml penicillin, 100 μg/ml streptomycin, 2 mM L-glutamine, and 1 mM sodium pyruvate, under standard incubator conditions (humidified atmosphere, 5% CO_2, 37°C). The hamster BHK cell line stably expressing the human *MRP1/ABCC1* gene, named BHK-MRP1, was a gift from Dr. Riordan (Mayo Clinic Arizona, S.C. Johnson Medical Research Center, Scottsdale, AZ) (Chang et al., 1997). These cells were grown as adherent monolayer cultures in Dulbecco's modified Eagle's medium/NUT mix F-12 (1:1) supplemented with 10% FCS, 100 U/ml penicillin, 100 μg/ml streptomycin, and 2 mM L-glutamine under standard incubator conditions (humidified atmosphere, 5% CO_2, 37°C). The cells were kept under selective pressure by growing them in the presence of 100 μM methotrexate. To disrupt the actin cytoskeleton, cells were treated with 10 μg/ml cytochalasin D or 10 μM latrunculin B for 35 min. In some cases, cells were preincubated with 10 μM nocodazole for 45 min to disrupt microtubules, followed by treatment with both nocodazole and latrunculin B for 35 min. On the other hand, cells were pre- and cotreated with 300 μM tyrphostin A23. In some experiments, cells were treated with 50 nM jasplakinolide for 20 h. All incubations with cytoskeleton modulators and all control experiments without these modulators were performed in medium without serum to avoid binding of the modulators to serum factors.

Isolation of Detergent-Free Lipid Rafts. Neuro-2a cells were plated at a density of 2×10^5 cells/ml and BHK-MRP1 at 2.5×10^5 cells/ml, 1 day before the experiment. Detergent-free lipid rafts were isolated as described previously (Macdonald and Pike, 2005). The whole procedure was performed on ice. In short, confluent cells of two 75-cm^2 flasks were washed with base buffer (20 mM Tris-HCl, pH 7.8, 250 mM sucrose) supplemented with 1 mM $CaCl_2$ and 1 mM $MgCl_2$. The cells were collected by scraping in this solution and centrifuged for 2 min at 250*g*. The resulting pellet was dissolved in 1 ml of base buffer supplemented with 1 mM $CaCl_2$, 1 mM $MgCl_2$, and protease inhibitors. After homogenization by passage through a 25-gauge needle 20 times, another centrifugation step for 10 min at 1000*g* followed. The resulting postnuclear supernatant (PNS) was collected and transferred to a separate tube. The pellet was homogenized again in 1 ml of base buffer supplemented with 1 mM $CaCl_2$, 1 mM $MgCl_2$, and protease inhibitors, sheared through the needle 20 times, and centrifuged. The second PNS was combined with the first. Protein content of the combined PNS was determined (Smith et al., 1985), and an equal amount of protein per sample was taken and adjusted to 2 ml of volume. Thereafter, 2 ml of base buffer containing 50% OptiPrep was added to this 2 ml of PNS. By using a gradient mixer, 8-ml gradient of 0 to 20% OptiPrep in base buffer was applied on top of this 4 ml in a centrifugation tube. After centrifugation for

Downloaded from molpharm.aspetjournals.org by guest on December 1, 2012

MOL PHARM

MOLECULAR PHARMACOLOGY

90 min at 22,000 rpm and 4°C in a Beckman SW41 rotor (Beckman Coulter, Inc., Fullerton, CA) nine fractions of 1.34 ml of were collected (from top to bottom) and stored at −80°C.

Immunoblot Analysis. Protein from equal volumes of the gradient fractions was trichloroacetic acid-precipitated and resuspended in sample buffer (5% SDS, 5% β-mercaptoethanol, 0.125M Tris-HCl, pH 6.8, and 40% glycerol). The samples were resolved on SDS-polyacrylamide gel electrophoresis (10%) minigels and subsequently electrotransferred onto a nitrocellulose membrane (Trans-Blot Transfer Medium membrane; Bio-Rad Laboratories, Hercules, CA). The membranes were rinsed with PBS and incubated (1 h at RT) with Odyssey blocking buffer/PBS [1:1 (v/v)]. Membranes were incubated (overnight at 4°C) with a primary antibody against MRP1 (ABCC1) (1:1000), Cav-1 (1:1000), or actin (1:5000) in Odyssey blocking buffer/PBS [1:1 (v/v)] containing 0.1% (v/v) Tween 20. Membranes were rinsed in washing buffer [PBS containing 0.1% (v/v) Tween 20] and subsequently incubated for 1 h with the appropriate infrared dye-conjugated secondary antibody (1:5000) (LI-COR Biosciences, Westburg, Leusden, The Netherlands) in Odyssey blocking buffer/PBS [1:1 (v/v)], containing 0.1% (v/v) Tween 20. After rinsing with washing buffer followed by PBS, the immunoblots were scanned with the Odyssey (LI-COR Biosciences) to visualize the immunoreactive complexes, according to the manufacturer's instructions. Relative quantification of the complexes was performed using the Odyssey software.

Analysis of Cholesterol, Sphingolipid, and Protein Content of OptiPrep Gradient Fractions. Lipids were extracted from pooled OptiPrep gradient fractions (Bligh and Dyer, 1959). In the extract, the cholesterol concentration was determined spectrophotometrically by a cholesterol oxidase/peroxidase assay (Gamble et al., 1978). Sphingolipids were analyzed by liquid chromatography-electrospray ionization tandem mass spectrometry on a PE-Sciex API 3000 triple quadrupole mass spectrometer equipped with a turbo ionspray source as described previously (Sullards and Merrill, 2001). High-performance liquid chromatography separation was performed as described previously (Sullards et al., 2003) with the following changes: an APS-2 Hypersil 150 × 2.1 mm column (Thermo Electron, Breda, The Netherlands) was used, and the flow rate was 200 μl/min. N_2 was used as the nebulizing gas and drying gas for the turbo ionspray source. The ion spray needle was held at 5500 V, and the orifice and ring voltages were kept low (30 and 150 V, respectively) to prevent collisional decomposition of molecular ions before entry into the first quadrupole; the orifice temperature was set to 500°C. N_2 was used to collisionally induce dissociations in Q2. Multiple reaction monitoring scans were acquired by setting Q1 and Q3 to pass the precursor and product ions of the most abundant sphingolipid molecular species. MRM transitions and collision energies for each species were taken from Table 1 in Sullards et al. (2003). The transitions correspond to ceramides, glucosylceramides, lactosylceramides, and sphingomyelins with a d18:1 sphingoid base (sphingosine) and C16:0, DHC16:0, C18:0, C20:0, C22:0, C24:1, C24:0, C26:1, and C26:0 fatty acids, respectively. Quantitation was achieved by spiking the samples before extraction with the C12-fatty acid homologs of ceramide, glucosylceramide, lactosylceramide, and sphingomyelin. The amounts of individual sphingolipid species were added to obtain the total sphingolipid pool. Protein content of pooled OptiPrep gradient fractions was determined as described by Smith et al. (1985).

Reverse Transcriptase-Polymerase Chain Reaction. Total RNA was isolated from cells by using RNeasy Mini Kit according to the manufacturer's instructions. Total RNA was isolated from murine liver and kidney using TRI reagent according to the manufacturer's instructions. Single-stranded cDNA was synthesized from 1 μg of RNA by using 0.5 μg of Oligo$(dT)_{12–18}$ primer, 200 U of Superscript RT, 4 μl of 5× First Strand buffer, 10 mM 1,4-dithiothreitol, and 0.5 mM each dNTP in a total volume of 20 μl. The RNA sample plus Oligo$(dT)_{12–18}$ primer were denatured at 65°C for 15 min and placed on ice for 5 min before adding it to the reaction. Reverse transcription was performed for 1 h at 37°C, and the samples were subsequently heated for 5 min at 99°C to terminate the reverse-transcription reaction. PCR was performed with Platinum Blue PCR SuperMix using 1 μl of the obtained cDNA and 250 nM each of the appropriate sense and antisense primers, according to the manufacturer's instructions. The final reaction volume was 25 μl. The tubes were incubated in a GeneAmp PCR System 9700 (PerkinElmer Life and Analytical Sciences, Waltham, MA) at 94°C for 5 min to denature the primers and cDNA. The cycling program was 94°C for 30 s, 55°C for 30 s, and 72°C for 45 s. The number of cycles was 35 for ABC transporters and 30 for β-actin. The following primer sequences were used [GenBank (GB) accession numbers and nucleotide positions in brackets]: Mrp1 sense (GB AF022908 [248–276]), 5′-GGCAGACCTCTTCTACTCT-3′, antisense (GB AF022908 [834–815]), 5′-GGCATACACAATCCGTACAG-3′ (576-bp amplified product); Mrp2 sense (GB BC172749 [268–292]), 5′-AGCCATAGACCTGTCTCTTGCACTC-3′, antisense (GB BC172749 [892–868]), 5′-GACAAGGACATCTTGGCTCTGACTC-3′ (624-bp amplified product); Mrp3 sense (GB BC150788 [227–248]), 5′-CATCAGCTCGGCTACATAGTCC-3′, antisense (GB BC150788 [799–778]), 5′-AGAGCAGTCCTCCTCAGACAGA-3′ (572-bp amplified product); Mrp4 sense (GB BC150822 [161–180]), 5′-ACTGGTCATAAGCGGAGACT-3′, antisense (GB BC150822 [476–457]), 5′-CGTAGCCATAAGCTGTATGC-3′ (315-bp amplified product); Mrp5 sense (GB BC090629 [264–285]), 5′-CAGGTTCCGGAGAACAAGATCG-3′, antisense (GB BC090629 [866–845]), 5′-GCAAGTGACCAGGAGCGTACAA-3′ (602-bp amplified product); Mrp6 sense (GB BC156560 [483–502]), 5′-GCATCTTGCCAGGAATCAAC-3′, antisense (GB BC156560 [833–814]), 5′-TGCAGCTTCTCCTCCATTCT-3′ (350-bp amplified product); Mrp7 sense (GB AF417121 [680–698]), 5′-CCTTCCTGTCCTCTGAGAG-3′, antisense (GB AF417121 [936–917]), 5′-GGCCAGGTAGCAACATCCAA-3′ (256-bp amplified product); Mdr1a sense (GB M33581 [255–274]), 5′-GTTATGCAGGTTGGCTAGAC-3′, antisense (GB M33581 [521–502]), 5′-CCTGGATGTAGGCAACTATG-3′ (266-bp amplified product); Mdr1b sense (GB BC141363 [241–260]), 5′-GGACAAGCTGTGCATGATTC-3′, antisense (GB BC141363 [426–407]), 5′-TCCAGACTGCTGTTGCTGAT-3′ (185-bp amplified product); and β-actin sense (GB M12481 [304–321]), 5′-AACACCCCAGCCATGTAC-3′, antisense (GB M12481 [557–540]), 5′-ATGTCACGCACGATTTCC-3′ (254-bp amplified product). Ten microliters of PCR product was loaded onto a 2% agarose gel stained with ethidium bromide.

Detection of Mrp1/MRP1 (Abcc1/ABCC1)-Mediated Efflux by Flow Cytometric Analysis. Neuro-2a cells were plated at a density of 2×10^5 cells/ml and BHK-MRP1 at 2.5×10^5 cells/ml, 1 day before the experiment. Cells were harvested by trypsinization, washed with HBSS, and incubated with the Mrp1/MRP1 (Abcc1/ABCC1) substrate 5-carboxyfluorescein diacetate (CFDA; 0.5 μM in HBSS) at 10°C for 60 min. Cells were transferred to ice and washed with ice-cold HBSS. In case of the time point 0-min samples, the Mrp1/MRP1 (Abcc1/ABCC1) inhibitor MK571 (20 μM) was added at this point. In other samples, to allow efflux, the cells were incubated at 37°C in absence of MK571 during various time intervals. In case of the inhibitor control, the 37°C incubation was performed in the presence of MK571. All subsequent steps were performed on ice. The efflux of the fluorescent substrate was stopped by ice-cold centrifugation, and the cells were resuspended in ice-cold HBSS containing MK571. On the other hand, in some experiments, Neuro-2a cells were incubated with the substrate rhodamine 123 (10 μM in HBSS), and the inhibitor cyclosporin A (10 μM) was used. The remaining cell-associated fluorescence was determined by flow cytometric analysis using an Elite flow cytometer (Beckman Coulter). For each sample, 5000 events were collected and analyzed using Win-list 5.0 software (Verity Software House Inc., Topsham, ME). With 5000 events, clear Gaussian fluorescence distributions were obtained with a calculated error of measurement of 1.4%. In all graphic representations of results, the values express the fluorescence remaining in the cells after a certain time window of efflux at 37°C as a percentage

Downloaded from molpharm.aspetjournals.org by guest on December 1, 2012

MOL PHARM

MOLECULAR PHARMACOLOGY

of the fluorescence after loading the cells (i.e., 100%). In the latter case, the cells were not allowed to efflux, because they were kept on ice. This was done for all conditions, so the values always indicate the fraction of the initial CFDA load that remains in the cells after a certain period of efflux at 37°C.

Confocal Laser-Scanning Fluorescence Microscopy. Neuro-2a cells were plated on glass coverslips in 12-well plates at a density of 7×10^4 cells/ml and BHK-MRP1 at 1.5×10^5 cells/ml, 1 day before the experiment. Cells were fixed with 4% paraformaldehyde at RT for 20 min, permeabilized with 0.1% Triton X-100 at RT for 5 min, and blocked with 2% FCS in PBS at RT for 30 min before antibody incubation. On the other hand, cells were fixed with cold (−20°C) methanol or acetone on ice for 5 min, washed extensively with PBS, and blocked with 2% FCS in PBS at RT for 30 min before antibody incubation. It should be noted that the latter protocol does not require a permeabilization step, because methanol and acetone readily permeabilize cells. Both fixation protocols were compared for all antigens to optimize the staining procedure for each antigen. For instance, MRP1 staining by primary and (fluorescent) secondary antibodies is much more pronounced after methanol fixation compared with paraformaldehyde fixation. Primary (overnight at 4°C) and secondary (2 h at RT) antibody incubations were carried out in PBS. Cells were stained with antibodies against MRP1 (ABCC1) (1:50), Cav-1 (1:100), transferrin receptor (1:100), giantin (1:500), or β-tubulin (1:100) and appropriate Alexa-conjugated secondary antibodies. On the other hand, F-actin was stained with Alexa 488- or 633-conjugated phalloidin. After incubations, cells were washed three times with PBS. Analysis of the samples was performed using a TCS Leica SP2 AOBS Confocal Laser Scanner Microscope (Leica, Wetzlar, Germany) equipped with an HCX PL APO 63 × 1.4 oil CS objective in combination with Leica Confocal Software. Images were processed using Adobe Photoshop CS3 (Adobe Systems, Mountain View, CA).

Results

Validation of the Model Cell Lines. This study aims to determine the effect of cortical actin on Mrp1/MRP1 (Abcc1/ABCC1) localization and function and relies on the use of two model cell lines that express active Mrp1 (Abcc1) or MRP1 (ABCC1). Neuro-2a cells express endogenous murine Mrp1 (Abcc1), whereas hamster BHK-MRP1 cells strongly express human MRP1 (ABCC1) as a result of transfection. If Mrp1/MRP1 (Abcc1/ABCC1) is sensitive to cortical actin disruption in both cell lines, this would indicate that the effect is not cell type-specific. We used CFDA as a substrate to measure Mrp1/MRP1 (Abcc1/ABCC1) activity. Its efflux from Neuro-2a cells (Fig. 1A) was effectively inhibited by the Mrp/MRP-specific inhibitor MK571. When using the Pgp (Abcb1) inhibitor cyclosporin A, less inhibition of CFDA efflux was observed in Neuro-2a cells (Fig. 1A). With the Pgp (Abcb1) substrate rhodamine 123, very little efflux activity was observed, and there was little or no effect of cyclosporin A or MK571 (Fig. 1A). This indicates that with CFDA as a substrate, we measure Mrp (Abcc) activity in these cells. With the CFDA assay, we cannot discriminate between various members of the Mrp (Abcc) subfamily. Therefore, we performed reverse transcriptase-polymerase chain reaction (RT-PCR) to analyze the Mrp (Abcc) mRNA expression profile in Neuro-2a cells. Of the seven subfamily members that were tested, Neuro-2a cells only expressed Mrp1 (Abcc1) (Fig. 1C). Thus, potential interfering effects of other Mrps (Abccs) in efflux assays using CFDA as a substrate are minimized. Moreover, in accordance with the absence of rhodamine 123 efflux, the two murine forms of Pgp (Abcb1) [i.e., Mdr1a (Abcb1a) and Mdr1b (Abcb1b)] were not expressed in Neuro-2a cells (Fig. 1C). In BHK-MRP1 cells, RT-PCR could not be performed because of the lack of cDNA sequence information of the Mrps (Abccs) in these hamster cells. However, because of the forced expression, BHK-MRP1 cells displayed a drastically higher level of MRP1 than the level of Mrp1 in Neuro-2a cells (Fig. 1D). Moreover, CFDA efflux from BHK-MRP1 cells was effectively inhibited by MK571 (Fig. 1B). Therefore, it is reasonable to assume that efflux of CFDA in these cells can be attributed to MRP1.

Cortical Actin Stabilizes Lipid Raft Localization and Function of Mrp1 (Abcc1) in Neuro-2a Cells. A large group of Neuro-2a cells was imaged at two different focal planes in the *z*-direction, one focal plane for visualization of stress fibers, and the other focal plane for visualization of cortical actin. The actin cytoskeleton is organized in such a way in these cells that the stress fibers occur mostly in the bottom part of the cells, in which the cells are attached to the glass coverslip. The stress fibers are typically long fibers that

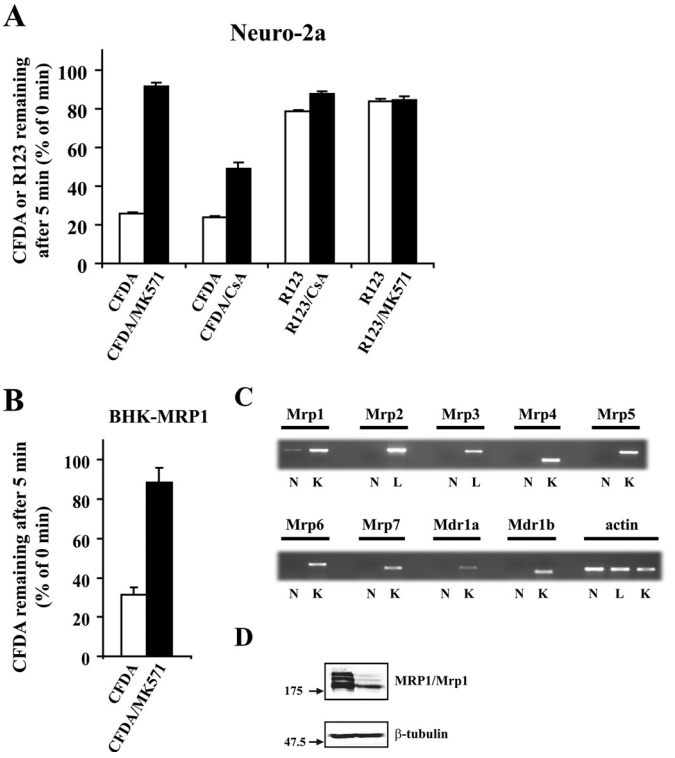

Fig. 1. Validation of the Mrp1/MRP1 model cell lines Neuro-2a and BHK-MRP1. A, the efflux activity of Mrp1 (Abcc1) during 5 min in Neuro-2a cells was measured under control conditions or upon inhibition by 20 μM MK571 or 10 μM cyclosporin A using CFDA as substrate. The same was done for the efflux activity of Pgp (Abcb1) using rhodamine 123 (R123) as substrate. The 5-min fluorescence values are expressed as the percentage of 0 min (=100%). Data represent the mean ± S.D. of three independent experiments. B, the efflux activity of MRP1 (ABCC1) during 5 min in BHK-MRP1 cells was measured under control conditions or upon inhibition by 20 μM MK571 using CFDA as substrate. The 5-min fluorescence values are expressed as the percentage of 0 min (=100%). Data represent the mean ± S.D. of three independent experiments. C, the mRNA expression profile of Mrp (Abcc) subfamily members 1 to 7 and the Pgp (Abcb1) variants Mdr1a (Abcb1a) and Mdr1b (Abcb1b) was analyzed by RT-PCR in Neuro-2a cells (N) and the positive controls murine liver tissue (L) and murine kidney tissue (K). D, the expression of MRP1 and Mrp1 protein in BHK-MRP1 and Neuro-2a cells, respectively, was analyzed by Western blotting using β-tubulin as loading control. Note that the same amount of protein (30 μg) of BHK-MRP1 cells loaded on gel results in a higher level of MRP1 compared with the level of Mrp1 in Neuro-2a cells.

Downloaded from molpharm.aspetjournals.org by guest on December 1, 2012

MOL PHARM

MOLECULAR PHARMACOLOGY

extend from one membrane anchor point to another membrane anchor point on the opposite side of the cell. Upward in the cells in *z*-direction, the cortical actin becomes apparent. The cortical actin is localized close to the plasma membrane to support the membrane and provide tension to the membrane. By focusing the confocal laser microscope on a *z*-layer close to the glass coverslip, we can image stress fibers in control Neuro-2a cells (Fig. 2B, arrowhead) and by focusing more up in the cells, we can image cortical actin (Fig. 2D, arrow). We used two modulators of the actin cytoskeleton, latrunculin B, and cytochalasin D. Treatment with 10 μM latrunculin B resulted in loss of both stress fibers and cortical actin (Fig. 2, F and H, respectively). As a control, to show that we indeed focused on the right *z*-layer, cells were stained for ezrin, which still is localized in the cortical region of the plasma membrane (Fig. 2G). Upon treatment with 10 μg/ml cytochalasin D, stress fibers were disrupted (Fig. 2L), but cortical actin was still present (Fig. 2N, arrow). Taken together, this shows that latrunculin B and cytochalasin D at the used concentrations affect cortical actin differently and make these two modulators valuable tools for studying the role of cortical actin in function and localization of Mrp1 (Abcc1).

We used a detergent-free method for the isolation of lipid rafts and first characterized the gradient fractions in terms of cholesterol and sphingolipid enrichment. For this purpose, fractions 1–2 were pooled, as well as 3–4, 5–6 and 7–9. Fractions 1 and 2 were most strongly enriched in both cholesterol and sphingolipids (Fig. 3) and, to a lesser extent, also fractions 3 and 4. This indicates that fractions 1 to 2, with the lowest buoyant density, optimally fulfil the criteria for lipid rafts. Latrunculin B, but not cytochalasin D, treatment resulted in a shift of Mrp1 (Abcc1) out of lipid raft fractions in Neuro-2a cells (Fig. 4A). Mrp1 (Abcc1) shifted from the lipid raft fractions 1 to 2 to the fractions 5 to 6, but mostly 7 to 9, all nonraft fractions (Fig. 4B). Also Cav-1, an established lipid raft marker, displayed a shift out of lipid raft fractions upon latrunculin B treatment but not upon cytochalasin D treatment (Fig. 4A). It is noteworthy that actin was partly localized in lipid raft fractions in control cells and also shifted from lipid rafts fractions in latrunculin B-treated but not in cytochalasin D-treated cells (Fig. 4A). Next, we measured the efflux activity of Mrp1 (Abcc1). Efflux kinetics were determined (Fig. 5A) and the efflux time of 5 min was chosen for all subsequent experiments on the affect of cytoskeleton modulators. Efflux inhibition by latrunculin B was concentration-

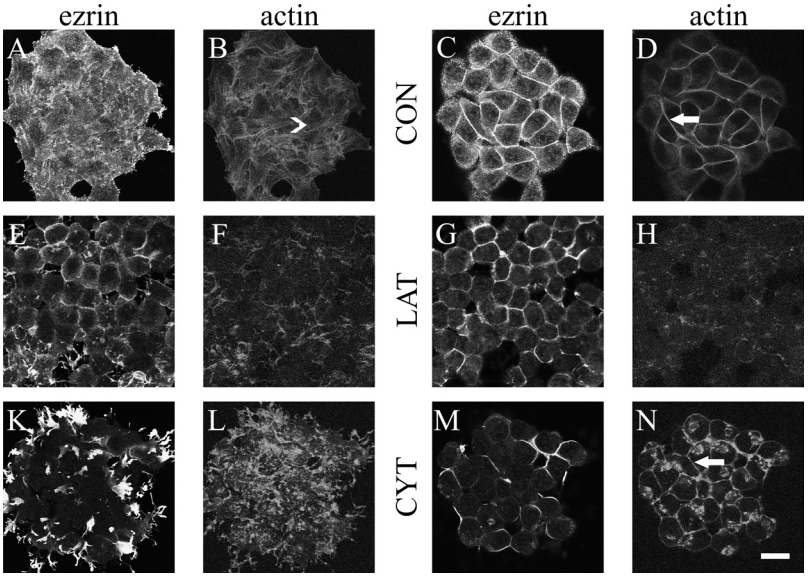

Fig. 2. Disruption of actin by cytochalasin D is limited to stress fibers, whereas latrunculin B also disrupts cortical actin in Neuro-2a cells. Neuro-2a cells were untreated (CON; A–D), treated with 10 μM latrunculin B (LAT; E–H), or treated with 10 μg/ml cytochalasin D (CYT; K–N). Cells were stained for ezrin (A, C, E, G, K, and M) or actin (B, D, F, H, L, and N). Left, images of a *z*-layer, when focused on stress fibers; right, the focus is on cortical actin in the same cells. Note that cortical actin (arrows) remains in cytochalasin D-treated cells but is lost in latrunculin B-treated cells. Stress fibers (arrowhead) are lost in both latrunculin B- and cytochalasin D-treated cells. Scale bar, 20 μm.

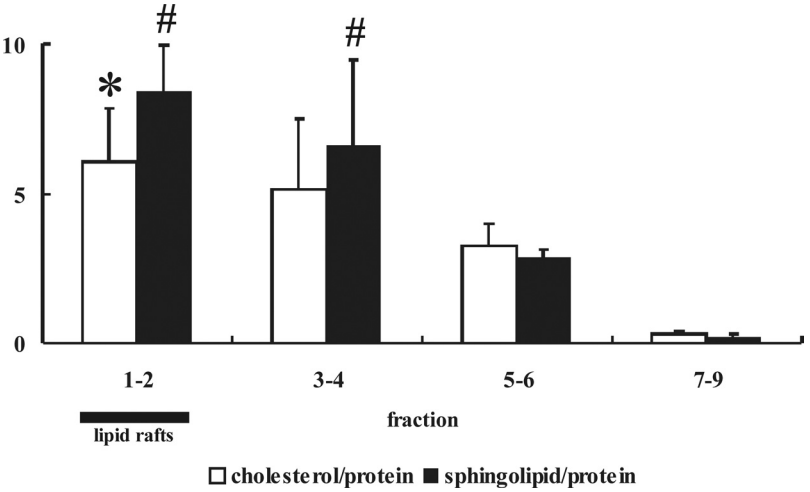

Fig. 3. Enrichment of cholesterol and sphingolipid relative to protein in detergent-free lipid raft gradients of Neuro-2a cells. Detergent-free lipid raft gradients were analyzed for cholesterol (□) and sphingolipid (■) profile. These lipid classes were measured in pooled gradient fractions and are expressed relative to protein content of the pooled gradient fractions. To calculate the ratios of cholesterol/protein and sphingolipid/protein, the values of percentages in the gradient of each cholesterol, sphingolipids, and protein were used. This ratio is therefore without unit and represents the relative enrichment in gradient fractions of cholesterol and sphingolipids, respectively, relative to protein enrichment in the respective fractions. Data represent the mean ± S.D. of three independent experiments. *, values are significantly ($P < 0.05$) different from the cholesterol/protein ratio of fractions 5 to 6 (nonlipid raft membrane fractions) as determined by Student's *t* test. #, values are significantly ($P < 0.05$) different from the sphingolipid/protein ratio of fractions 5 to 6 (nonlipid raft membrane fractions) as determined by Student's *t* test.

Downloaded from molpharm.aspetjournals.org by guest on December 1, 2012

dependent (Fig. 5B), and 10 μM was taken for subsequent experiments. Concomitant with a shift of Mrp1 (Abcc1) out of lipid rafts, its efflux function was reduced by latrunculin B treatment (Fig. 5C). Although latrunculin B strongly reduced Mrp1 (Abcc1)-mediated efflux, cytochalasin D was much less effective (Fig. 5C). As a control experiment, we tested whether the agent latrunculin B inhibited Mrp1 efflux function as a direct competitive inhibitor (DCI). In this case, Neuro-2a cells were not preincubated at 37°C with latrunculin B, but the actin modulator was administered during the CFDA substrate loading period at 10°C (DCI 1). On the other hand, latrunculin B was added just before the efflux commenced (DCI 2). Under both conditions, latrunculin B could not exert its effect through actin modulation, but only by direct inhibition of Mrp1 function. However, loss of Mrp1 function was not observed (Fig. 5D). Taken together, these results indicate that both Mrp1 (Abcc1) localization in lipid rafts and its functional activity as an efflux pump are dependent on intact cortical actin.

Cortical Actin Dependence of Mrp1/MRP1 (Abcc1/ABCC1) Localization and Function Is Not Cell Type-Specific. In BHK-MRP1 cells, a cell line that highly expresses human MRP1 (ABCC1), a similar effect of latrunculin B on MRP1 (ABCC1) localization in lipid raft fractions was observed (Fig. 6A). MRP1 (ABCC1) shifted from the lipid raft fractions 1 to 2 to the nonraft fractions 5 to 6 (Fig. 6B). Moreover, MRP1 (ABCC1)-mediated efflux was reduced by latrunculin B (Fig. 7A). Again, cytochalasin D had a minor effect on both localization in lipid raft fractions and efflux function of MRP1 (ABCC1) (Figs. 6, A and B, and 7A). Control BHK-MRP1 cells displayed stress fibers and cortical actin (Fig. 8A). Latrunculin B (Fig. 8C), but not cytochalasin D (Fig. 8B), caused disruption of cortical actin. When BHK-MRP1 cells were treated with latrunculin B for 35 min, washed, and further incubated for 15 h in FCS-containing medium without latrunculin B, the actin cytoskeleton recovered (Fig. 8D), and the cells displayed normal cell morphology and growth behavior. Concomitantly, the efflux activity of MRP1 (ABCC1) completely recovered (Fig. 7A). Finally, jasplakinolide was used to stabilize the actin cytoskeleton. BHK-MRP1 cells treated for 20 h in medium without serum including this actin modulator showed normal morphology, stress fibers, and cortical actin (Fig. 8F) compared with control cells that had been incubated for 20 h in medium without serum (Fig. 8E). In addition, jasplakinolide-treated cells displayed an accumulation of actin aggregates in the perinuclear region of the cells (Fig. 8F). Upon jasplakinolide treatment, MRP1 (ABCC1)-mediated efflux was enhanced, opposite to the effect of latrunculin B (Fig. 7B). In Neuro-2a cells, a similar trend was observed, but this effect was not significant (data not shown). MRP1 (ABCC1) association with lipid raft fractions was normal in jasplakinolide-treated BHK-MRP1 cells compared with control cells (Fig. 6, A and B). Taken together, these results indicate that the effects of cortical actin on both Mrp1/MRP1 (Abcc1/ABCC1) localization in lipid rafts and its functional activity as an efflux pump are not cell type-specific but occur in two different cell lines, Neuro-2a and BHK-MRP1, and thus can be generalized.

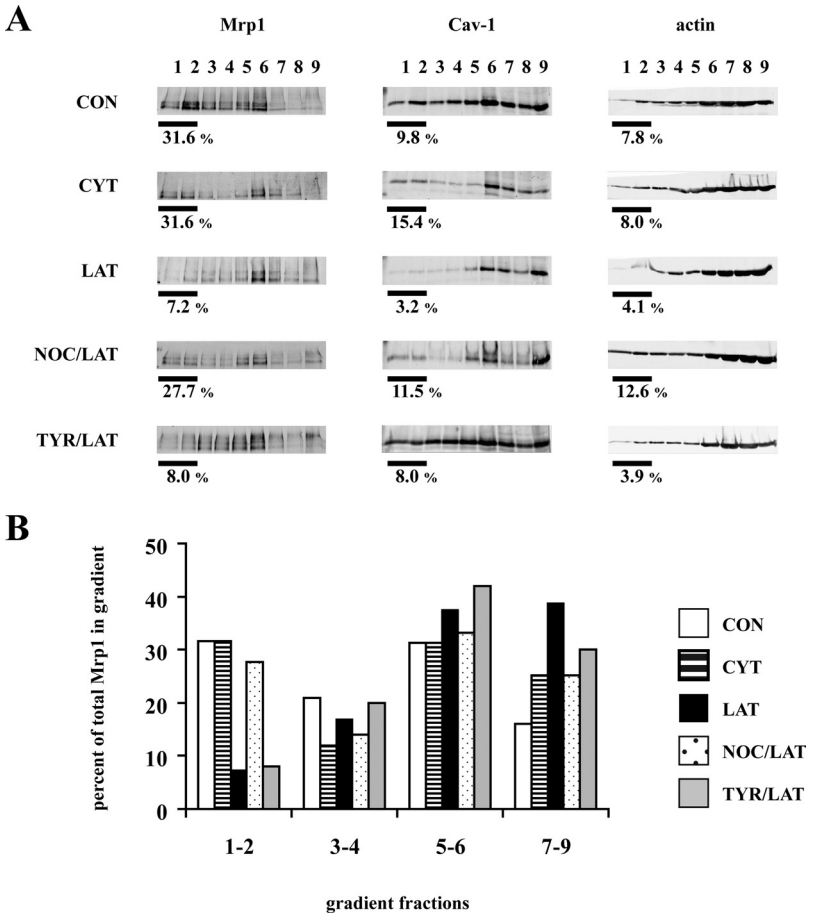

Fig. 4. Disruption of cortical actin results in loss of lipid raft association of Mrp1 (Abcc1) in Neuro-2a cells. Neuro-2a cells were untreated (CON), treated with 10 μg/ml cytochalasin D (CYT), with 10 μM latrunculin B (LAT), with 10 μM nocodazole followed by 10 μM nocodazole + 10 μM latrunculin B (NOC/LAT), or with 300 μM tyrphostin A23 followed by 300 μM tyrphostin A23 + 10 μM latrunculin B (TYR/LAT). A, lipid raft association of Mrp1 (Abcc1), Cav-1, and actin was analyzed under these conditions. The values indicate the percentage of the specific protein found in the lipid raft fractions (1–2), relative to the total of that protein in the entire gradient (nine fractions). Typical results taken from three independent experiments are shown. B, quantification of the distribution of Mrp1 (Abcc1) over the gradient fractions under these conditions.

MOL PHARM
MOLECULAR PHARMACOLOGY
aspet
Downloaded from molpharm.aspetjournals.org by guest on December 1, 2012

MOL PHARM

MOLECULAR PHARMACOLOGY

Cortical Actin Disruption Leads to Intracellular Accumulation of Mrp1/MRP1 (Abcc1/ABCC1). So far we have established that latrunculin B reduces efflux activity of Mrp1/MRP1 (Abcc1/ABCC1), and this effect seems to be correlated with a shift of Mrp1/MRP1 (Abcc1/ABCC1) out of lipid rafts. To further investigate the subcellular localization of the ABC transporter under these conditions, we used confocal microscopy. In control Neuro-2a cells, Mrp1 (Abcc1) is exclusively detected in the plasma membrane (Fig. 9a, A and D). Here, Mrp1 (Abcc1) seems to partly colocalize with actin (Fig. 9a, A–C), but not with Cav-1 (Fig. 9a, D–F). After latrunculin B treatment, there is still strong plasma membrane staining of Mrp1 (Abcc1), but in addition, some intracellular Mrp1 (Abcc1) is detected in the cell center (Fig. 9a, L). This was not observed after cytochalasin D treatment (Fig. 9a, G), in which Mrp1 (Abcc1) was detected exclusively in the plasma membrane and partly colocalized with actin (Fig. 9a, G–K). Upon incubation with latrunculin B, Cav-1 displayed pronounced intracellular staining in the cell center (Fig. 9a, M). Here, Mrp1 (Abcc1) and Cav-1 seemed to colocalize (Fig. 9a, L–N). Apparently, intact cortical actin prevented intracellular appearance of Mrp1 (Abcc1) and accumulation of Cav-1. Similar results were obtained in BHK-MRP1 cells, in which both MRP1 (ABCC1) and Cav-1 displayed increased intracellular staining upon latrunculin B treatment (Fig. 9b, G–K) but not upon cytochalasin D treatment (Fig. 9b, D–F). However, in control BHK-MRP1 cells, some intracellular MRP1 (ABCC1) (and Cav-1) staining was readily observed (Fig. 9b, A–C), in contrast to control Neuro-2a cells. This may be related to the forced expression of human MRP1 (ABCC1) in BHK-MRP1 cells. In view of these observations, we continued our studies regarding Mrp1 (Abcc1) localization in Neuro-2a cells.

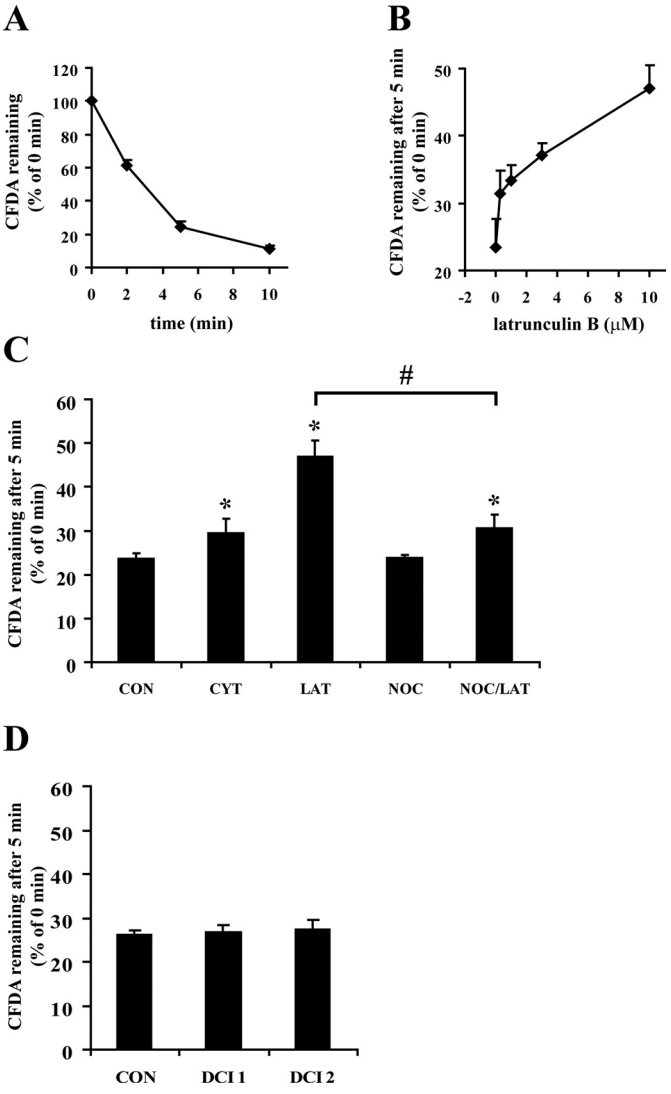

Fig. 5. Disruption of cortical actin results in reduced efflux function of Mrp1 (Abcc1) in Neuro-2a cells. Neuro-2a cells were untreated (CON), treated with 10 μg/ml cytochalasin D (CYT), with 10 μM latrunculin B (LAT), with 10 μM nocodazole (NOC), or with 10 μM nocodazole followed by 10 μM nocodazole + 10 μM latrunculin B (NOC/LAT). A, efflux kinetics of CFDA in control Neuro-2a cells. The fluorescence values after various periods of efflux are expressed as the percentage of 0 min (= 100%). Data represent the mean ± S.D. of three independent experiments. B, concentration-dependent effect of latrunculin B on Mrp1 (Abcc1)-mediated efflux of CFDA during 5 min in Neuro-2a cells. The 5-min fluorescence values are expressed as the percentage of 0 min (=100%). Data represent the mean ± S.D. of three independent experiments. C, the efflux activity of Mrp1 (Abcc1) during 5 min was measured under conditions of cytoskeletal modulation using CFDA as substrate. The 5-min fluorescence values are expressed as the percentage of 0 min (=100%). Data represent the mean ± S.D. of three independent experiments. *, values that are significantly different from control ($P < 0.05$, as determined by Student's t test). #, efflux of NOC/LAT-treated cells is significantly different from that of LAT-treated cells ($P < 0.05$, as determined by Student's t test). D, the efflux activity of Mrp1 (Abcc1) during 5 min was measured under conditions of potential DCI by latrunculin B. Latrunculin B was added during the CFDA loading period at 10°C (DCI 1) or alternatively just before the efflux period commenced (DCI 2). The 5-min fluorescence values are expressed as the percentage of 0 min (=100%). Data represent the mean ± S.D. of three independent experiments. DCI 1 and DCI 2 values are not significantly different from control ($P > 0.05$, as determined by Student's t test).

Intracellular Localization of Mrp1 (Abcc1) Is Due to Increased Endocytosis. To investigate whether intracellu-

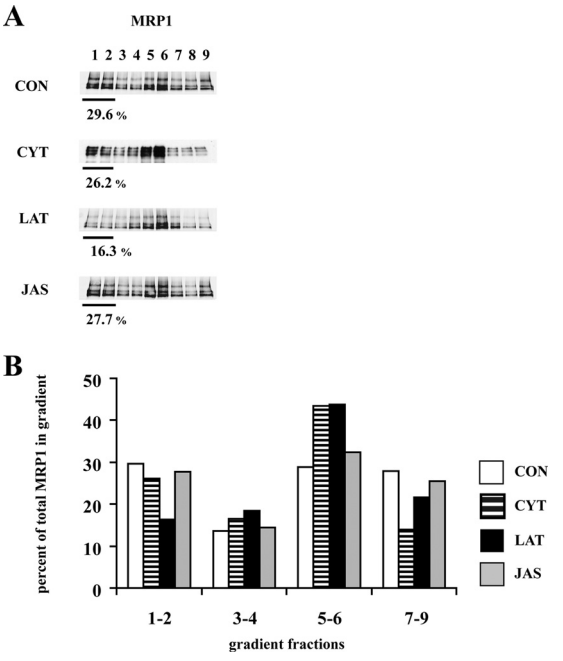

Fig. 6. Disruption of cortical actin results in loss of lipid raft association of MRP1 (ABCC1) in BHK-MRP1 cells. BHK-MRP1 cells were untreated (CON), treated with 10 μg/ml cytochalasin D (CYT) for 35 min, with 10 μM latrunculin B (LAT) for 35 min, or with 50 nM jasplakinolide (JAS) for 20 h in medium without serum. A, lipid raft association of MRP1 (ABCC1) was analyzed under various conditions. The values indicate the percentage of MRP1 (ABCC1) found in the lipid raft fractions (1–2) relative to the total of that protein in the entire gradient (nine fractions). Typical results taken from three independent experiments are shown. B, quantification of the distribution of MRP1 (ABCC1) over the gradient fractions under these conditions.

Downloaded from molpharm.aspetjournals.org by guest on December 1, 2012

MOL PHARM
MOLECULAR PHARMACOLOGY
aspet

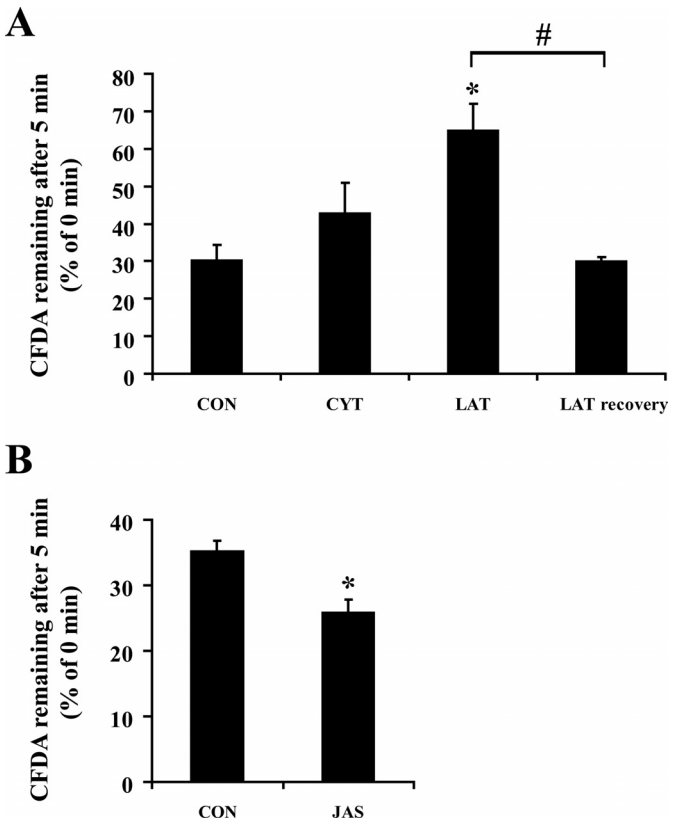

Fig. 7. Disruption of cortical actin results in reduced efflux function of MRP1 (ABCC1) in BHK-MRP1 cells. BHK-MRP1 cells were untreated (CON), treated with 10 μg/ml cytochalasin D (CYT) for 35 min, with 10 μM latrunculin B (LAT) for 35 min, or with 50 nM jasplakinolide (JAS) for 20 h in medium without serum. LAT-treated cells were allowed to recover (LAT recovery) for 15 h in FCS-containing medium in the absence of latrunculin B. A, the efflux activity of MRP1 (ABCC1) during 5 min was measured under various conditions using CFDA as substrate. The 5-min fluorescence values are expressed as the percentage of 0 min (= 100%). Data represent the mean ± S.D. of three independent experiments. *, values that are significantly different from control ($P < 0.05$, as determined by Student's t test). #, efflux of the recovered LAT-treated cells is significantly different from that of LAT-treated cells ($P < 0.05$, as determined by Student's t test). B, the efflux activity of MRP1 (ABCC1) during 5 min was measured in jasplakinolide-treated cells and compared with the respective control (i.e., cells incubated in medium without serum for 20 h). The 5-min fluorescence values are expressed as the percentage of 0 min (=100%). Data represent the mean ± S.D. of three independent experiments. *, efflux of JAS-treated cells is significantly higher than efflux of control cells ($P < 0.05$, as determined by Student's t test).

lar accumulation of Mrp1 (Abcc1) and Cav-1 was due to increased internalization of the proteins from the plasma membrane or alternatively impaired transport from the Golgi apparatus to the plasma membrane, we performed the following three experiments. First, immunolocalization with established markers for either Golgi (giantin) or endosomes (transferrin receptor) showed that intracellular Mrp1 (Abcc1) in latrunculin B-treated cells partly colocalized with the transferrin receptor (Fig. 10, A–C) but not with giantin (Fig. 10, D–F). This indicated that intracellular Mrp1 (Abcc1) was not a result of impaired transport out of the Golgi. Second, latrunculin B-treated cells were pretreated and cotreated with 10 μM nocodazole to disrupt microtubules. If intracellular Mrp1 (Abcc1) originated from impaired exit from the Golgi, the intracellular labeling pattern would stabilize, given that biosynthetic trafficking from the Golgi apparatus to the plasma membrane is microtubule-dependent. However, intracellular Mrp1 (Abcc1) was not detected (Fig. 11a, D), and Cav-1 did not accumulate in the cell center (Fig. 11a, H). The labeling pattern of Mrp1 (Abcc1) and Cav-1 resembled that of control cells (Fig. 11a, A and E, respectively) as well as cells treated with 10 μM nocodazole (Fig. 11a, C and G) and was largely different from that in latrunculin B-treated cells (Fig. 11a, B and F). In addition, this result indicated that intracellular Mrp1 (Abcc1) localization was not due to impaired Golgi to plasma membrane trafficking. Rather, nocodazole pretreatment prevented internalization of Mrp1 (Abcc1). Finally, to confirm endocytosis as the mechanism underlying intracellular localization of Mrp1 (Abcc1) in latrunculin B-treated cells, tyrphostin A23 was used to inhibit the process of endocytosis. When latrunculin B-treated Neuro-2a cells were pre- and coincubated with 300 μM tyrphostin A23, intracellular staining of Mrp1 (Abcc1) and Cav-1 was indeed not observed (Fig. 12a, D and H, respectively). The labeling pattern resembled that of control cells (Fig. 12a, A and E) as well as cells treated with 300 μM tyrphostin A23 (Fig. 12a, C and G) and was largely different from that in latrunculin B-treated cells (Fig. 12a, B and F). Taken together, these results indicate that latrunculin B-induced intracellular localization of Mrp1 (Abcc1) is due to increased endocytosis of the transporter from the plasma membrane.

Lipid Rafts Association, Plasma Membrane Localization, and Efflux Function of Mrp1 (Abcc1) Are Coupled and Depend on Intact Cortical Actin. As indicated, nocodazole pretreatment seemed to prevent latrunculin B-in-

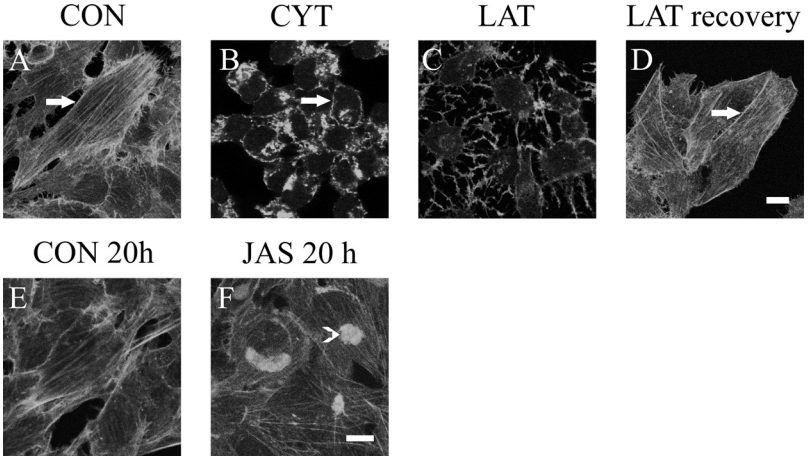

Fig. 8. Latrunculin reversibly disrupts cortical actin in BHK-MRP1 cells. BHK-MRP1 cells were untreated (CON), treated with 10 μg/ml cytochalasin D (CYT) for 35 min, with 10 μM latrunculin B (LAT) for 35 min, or with 50 nM jasplakinolide (JAS) for 20 h in medium without serum. LAT-treated cells were allowed to recover (LAT recovery) for 15 h in FCS-containing medium in the absence of latrunculin B. Cells were stained for actin. Cortical actin (arrows) remains in cytochalasin D-treated cells (B) but is lost in latrunculin B-treated cells (C). Cells that have recovered from latrunculin B treatment (D), as well as jasplakinolide-treated cells (F), display normal morphology, stress fibers, and cortical actin. Jasplakinolide-treated cells (F) in addition have accumulation of actin aggregates in the perinuclear region (arrowhead). Scale bars, 10 μm.

Downloaded from molpharm.aspetjournals.org by guest on December 1, 2012

MOL PHARM
MOLECULAR PHARMACOLOGY
aspet

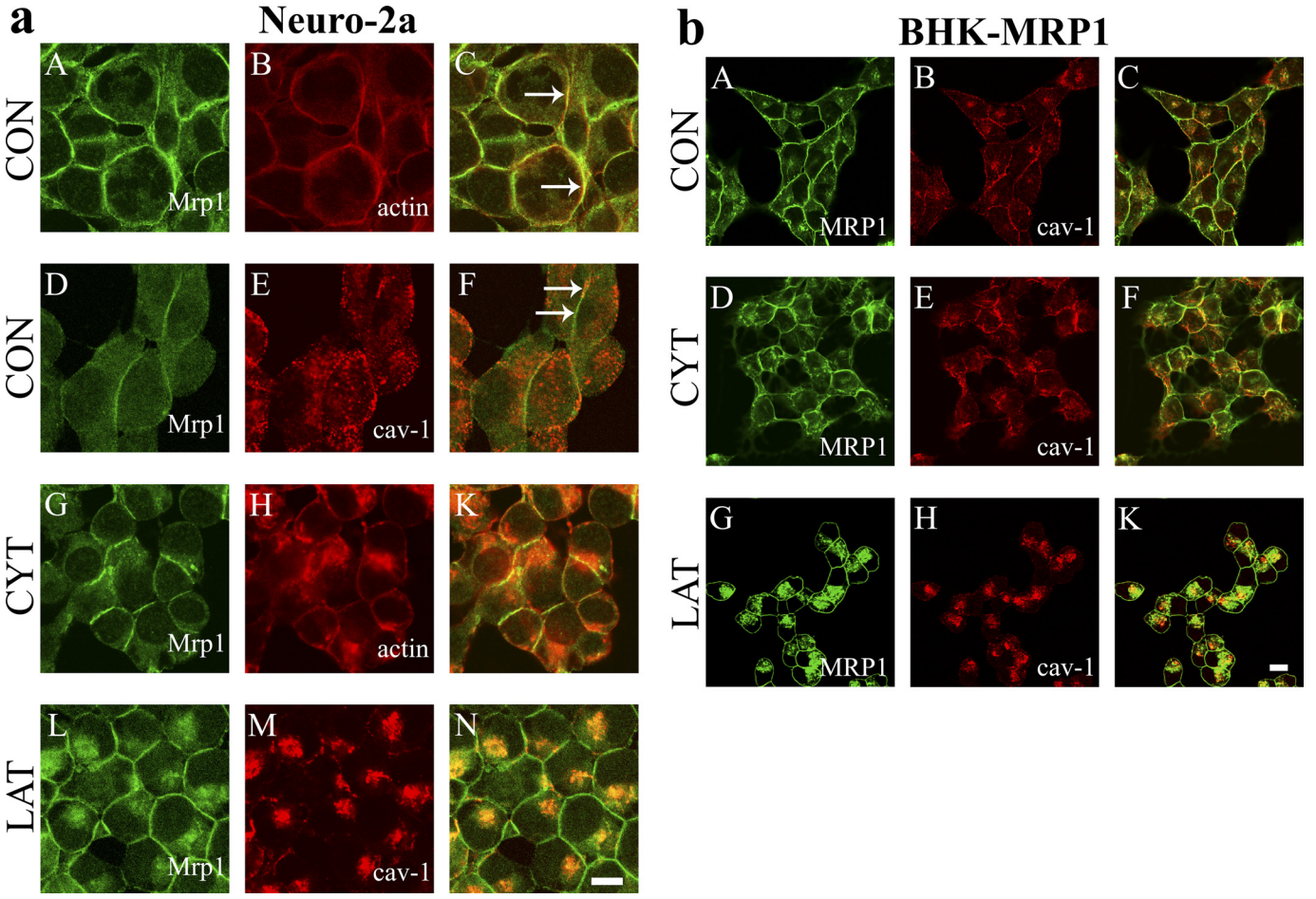

Fig. 9. a, disruption of cortical actin results in internalization of Mrp1 (Abcc1) as well as the lipid raft marker Cav-1 in Neuro-2a cells. Neuro-2a cells were untreated (CON; A–F), treated with 10 μg/ml cytochalasin D (CYT; G–K), or treated with 10 μM latrunculin B (LAT; L–N). Cellular localization of Mrp1 (Abcc1) (A, D, G, and L), actin (B and H), or Cav-1 (E and M) was analyzed by confocal microscopy under these conditions. C, F, K, and N are the overlay images. In latrunculin B-treated cells (L), but not cytochalasin D-treated cells (G), Mrp1 (Abcc1) displays intracellular staining, in which it seems to partly colocalize with Cav-1 (L-N). In control cells, Mrp1 (Abcc1) partly colocalizes with actin (arrows in C), but not with Cav-1 [arrows in F indicate either Mrp1 (Abcc1) or Cav-1]. Scale bar, 10 μm. b, disruption of cortical actin results in internalization of MRP1 (ABCC1) and the lipid raft marker Cav-1 in BHK-MRP1 cells. BHK-MRP1 cells were untreated (CON; A–C), treated with 10 μg/ml cytochalasin D (CYT; D–F), or treated with 10 μM latrunculin B (LAT; G–K). Cellular localization of MRP1 (ABCC1) (A, D, and G) or Cav-1 (B, E, and H) was analyzed by confocal microscopy under these conditions. (C, F, and K) are the overlay images. In latrunculin B-treated cells (G), but not cytochalasin D-treated cells (D), MRP1 (ABCC1) displays enhanced intracellular staining, in which it partly colocalizes with Cav-1 (G–K). In control cells, MRP1 (ABCC1) does not colocalize with Cav-1 in the plasma membrane (A–C). In contrast to control Neuro-2a cells (Fig. 9aA), control BHK-MRP1 cells display some intracellular MRP1 (ABCC1) staining in the cell center (Fig. 9bA). Scale bar, 10 μm.

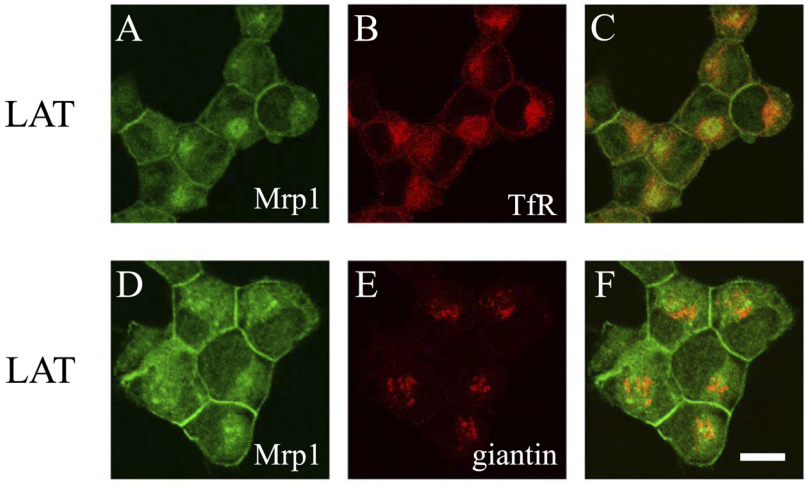

Fig. 10. Intracellular Mrp1 (Abcc1) partly colocalizes with transferrin receptor but not with giantin in Neuro-2a cells. Neuro-2a cells were treated with 10 μM latrunculin B (LAT). Cellular localization of Mrp1 (Abcc1) (A and D), transferrin receptor (TfR; B), or giantin (E) was analyzed by confocal microscopy under these conditions. C and F are the overlay images. Scale bar, 10 μm.

Downloaded from molpharm.aspetjournals.org by guest on December 1, 2012

duced internalization of Mrp1 (Abcc1). In accordance, under these conditions of combined treatment, lipid raft association of Mrp1 (Abcc1) was largely intact and comparable with that in control cells (Fig. 4, A and B). Moreover, with the combined treatment, the efflux activity of Mrp1 (Abcc1) was comparable with that in control cells and substantially different from that in latrunculin B-treated cells (Fig. 5C). It was therefore important to study the cortical actin status under these conditions. When applied separately, nocodazole disrupted microtubules without affecting cortical actin (Fig. 11b, C and G versus A and E), and latrunculin B disrupted cortical actin without affecting microtubules (Fig. 11b, B and F versus A

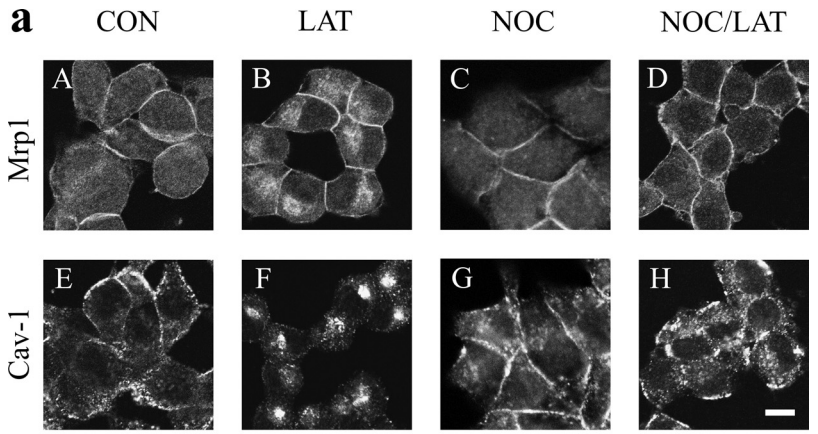

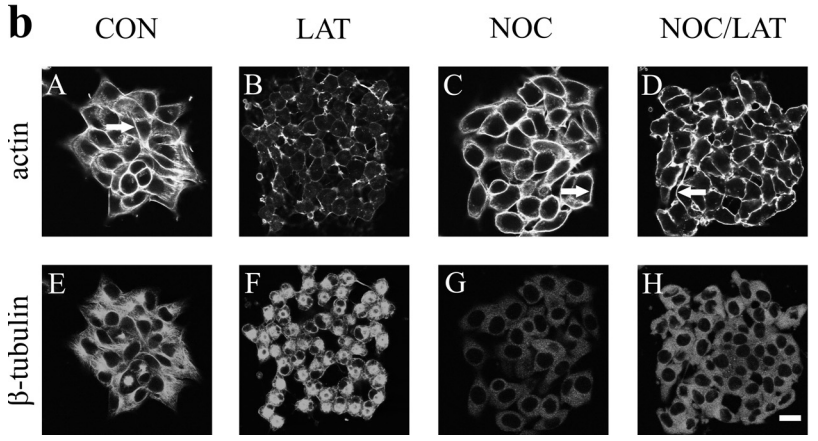

Fig. 11. a, Mrp1 (Abcc1) and Cav-1 do not accumulate intracellularly in latrunculin B-treated cells after pretreatment with nocodazole in Neuro-2a cells. Neuro-2a cells were untreated (CON; A and E), treated with 10 μM latrunculin B (LAT; B and F), treated with 10 μM nocodazole (NOC; C and G), or treated with 10 μM nocodazole followed by 10 μM nocodazole + 10 μM latrunculin B (NOC/LAT; D and H). Cellular localization of Mrp1 (Abcc1) (A–D) or Cav-1 (E–H) was analyzed by confocal microscopy under these conditions. Scale bar, 10 μm. b, cortical actin is not disrupted in latrunculin B-treated cells after pretreatment with nocodazole in Neuro-2a cells. Neuro-2a cells were untreated (CON; A and E), treated with 10 μM latrunculin B (LAT; B and F), 10 μM nocodazole (NOC; C and G), or 10 μM nocodazole followed by 10 μM nocodazole + 10 μM latrunculin B (NOC/LAT; D and H). Cells were stained for actin (A–D) and β-tubulin (E–H). The focus was on cortical actin in these cells. Note that cortical actin (arrows) remains in latrunculin B-treated cells after pretreatment with nocodazole. Scale bar, 20 μm.

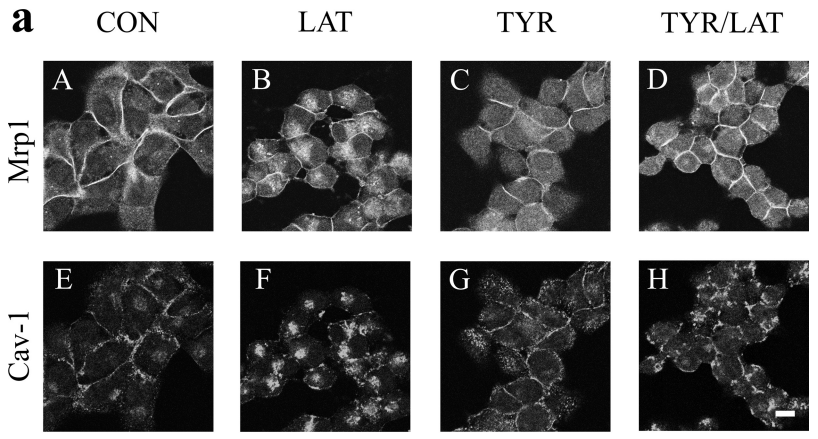

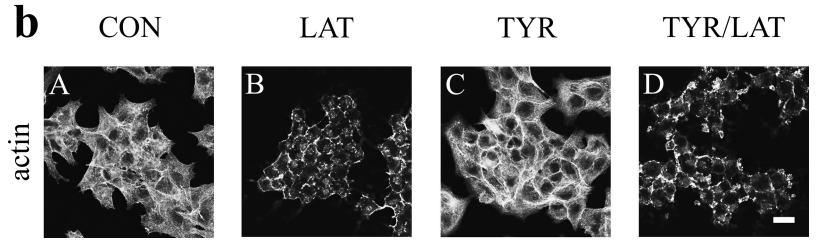

Fig. 12. a, Mrp1 (Abcc1) and Cav-1 do not accumulate intracellularly in latrunculin B-treated cells after pretreatment with tyrphostin A23 in Neuro-2a cells. Neuro-2a cells were untreated (CON; A and E), treated with 10 μM latrunculin B (LAT; B and F), treated with 300 μM tyrphostin A23 (TYR; C and G), or treated with 300 μM tyrphostin A23 followed by 300 μM tyrphostin A23 + 10 μM latrunculin B (TYR/LAT; D and H). Cellular localization of Mrp1 (Abcc1) (A–D) or Cav-1 (E–H) was analyzed by confocal microscopy under these conditions. Scale bar, 10 μm. b, tyrphostin A23 does not prevent latrunculin B-induced loss of cortical actin. Neuro-2a cells were untreated (CON; A), treated with 10 μM latrunculin B (LAT; B), 300 μM tyrphostin A23 (TYR; C), or 300 μM tyrphostin A23 followed by 300 μM tyrphostin A23 + 10 μM latrunculin B (TYR/LAT; D). Cells were stained for actin. Note that cortical actin is disrupted in latrunculin B-treated cells (B) and after pretreatment with tyrphostin A23 (D). In tyrphostin A23-treated cells, cortical actin and stress fibers are intact (C), as in control cells (A). Scale bar, 20 μm.

MOL PHARM
MOLECULAR PHARMACOLOGY
aspet
Downloaded from molpharm.aspetjournals.org by guest on December 1, 2012

MOL PHARM

MOLECULAR PHARMACOLOGY

and E). It is noteworthy that latrunculin B-treatment in combination with nocodazole and after nocodazole pretreatment did not result in the disruption of cortical actin (Fig. 11b, D and H), but stress fibers were still sensitive to the inhibitor (data not shown). Moreover, actin-lipid raft association under these conditions was comparable with control (Fig. 4A).

Tyrphostin A23 Prevents Latrunculin B-Induced Mrp1 (Abcc1) Internalization but Not Reduced Lipid Raft Association and Efflux Activity of the ABC Transporter. Tyrphostin A23 was able to prevent latrunculin B-induced internalization of Mrp1 (Abcc1) (Fig. 12a). It is noteworthy that this inhibitor of endocytosis was ineffective in preventing the other effects of latrunculin: under the conditions of combined tyrphostin A23/latrunculin B treatment, lipid raft association of Mrp1 (Abcc1) was reduced and comparable with that in latrunculin B-treated cells (Fig. 4, A and B). Tyrphostin A23 by itself somewhat reduced Mrp1 (Abcc1)-mediated efflux activity but could not prevent the stronger latrunculin B-mediated effect on Mrp1 (Abcc1) activity (Fig. 13). As expected, when latrunculin B-treated Neuro-2a cells were pre- and coincubated with 300 μM tyrphostin A23 (Fig. 12b, D), the actin-labeling pattern resembled that of latrunculin B-treated cells (Fig. 12b, B). This indicated that pre- and cotreatment with tyrphostin A23 did not prevent latrunculin B-induced loss of cortical actin. Moreover, lipid raft association of actin was reduced under these conditions, comparable with the situation in cells that had been treated with latrunculin B alone (Fig. 4A). In tyrphostin A23-treated cells, cortical actin and also stress fibers remained intact (Fig. 12b, C), as in control cells (Fig. 12b, A).

Discussion

In this study, we have shown for the first time that cortical actin is involved in stabilizing Mrp1/MRP1 (Abcc1/ABCC1) in lipid rafts on the cell surface of two cell lines, Neuro-2a and BHK-MRP1. Neuro-2a cells have endogenous expression of Mrp1 (ABCC1) but not the related Mrp (Abcc) subfamily members 2 to 7. BHK-MRP1 is a cell line that stably expresses human MRP1 (ABCC1). In contrast to cytochalasin D, latrunculin B caused the disruption of cortical actin, which is in agreement with other studies (e.g., Spector et al., 1999) and loss of actin from lipid raft fractions. This resulted in a shift of Mrp1/MRP1 (Abcc1/ABCC1) out of lipid raft fractions and its internalization by endocytosis. Similar events were recorded for the lipid raft marker Cav-1. These were probably separate events, because Mrp1/MRP1 (Abcc1/ABCC1) did not seem to colocalize with Cav-1: Mrp1/MRP1 (Abcc1/ABCC1) displayed continuous fluorescence in the plasma membrane, whereas Cav-1 presented with punctate fluorescence. This is in accordance with previous studies showing that ABC transporters are found in noncaveolar lipid rafts (Hinrichs et al., 2004; Radeva et al., 2005). Apparently, cortical actin was acting as a fence keeping raft-associated proteins from internalizing by endocytosis. For Cav-1, similar observations have been reported (Mundy et al., 2002). Inward budding of membranes leading to the formation of endocytic vesicles, may well be stimulated by the loss of cortical actin, which normally confers elasticity on the plasma membrane (Ananthakrishnan et al., 2006).

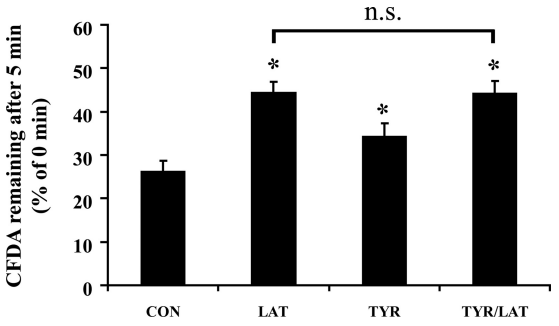

Fig. 13. Tyrphostin A23 does not prevent latrunculin B-induced reduction of MRP-mediated efflux activity. Neuro-2a cells were untreated (CON), treated with 10 μM latrunculin B (LAT), 300 μM tyrphostin A23 (TYR), or 300 μM tyrphostin A23 followed by 300 μM tyrphostin A23 + 10 μM latrunculin B (TYR/LAT). The efflux activity of Mrp1 (Abcc1) during 5 min was measured under conditions of cytoskeleton and endocytosis modulation using CFDA as substrate. The 5-min fluorescence values are expressed as the percentage of 0 min (=100%). Data represent the mean ± S.D. of three independent experiments. *, values that are significantly different from control ($P < 0.05$, as determined by Student's t test). n.s., efflux of TYR/LAT-treated cells is not significantly different from that of LAT-treated cells ($P > 0.05$, as determined by Student's t test).

The Mrp1/MRP1 (Abcc1/ABCC1) activity is reduced concomitant with a shift out of lipid rafts and internalization of the ABC transporter. This suggests that lipid raft-cortical actin complexes provide the cell with a mechanism to stabilize Mrp1/MRP1 (Abcc1/ABCC1) function. We have shown this in Neuro-2a cells, which express endogenous (murine) Mrp1 and extended our observations to a different cell line, BHK-MRP1, which expresses human MRP1. In this context, previous studies have provided evidence for a functional link between actin and two other ABC transporters [i.e., PGP (ABCB1) and MRP2 (ABCC2)] (Kikuchi et al., 2002; Luciani et al., 2002; Bacso et al., 2004). Therefore, actin association becomes a general theme in ABC transporter biology and may open new avenues for future therapeutic strategies to overcome MDR.

Our results obtained with nocodazole pretreatment have three important implications. First, they provide additional evidence that the intracellular accumulation of Mrp1 (Abcc1) in latrunculin B-treated cells is due to endocytosis and not to hampered biosynthetic transport out of the Golgi apparatus. Second, they provide additional evidence for the specific role of cortical actin in stabilizing Mrp1 (Abcc1) localization and function: all effects of latrunculin B treatment on Mrp1 (Abcc1) localization and function were prevented by nocodazole pretreatment, because cortical actin was not disrupted under these conditions. Moreover, it shows that the effects of latrunculin B on Mrp1 (Abcc1) can not be attributed to a general toxic effect of latrunculin B, because this toxic effect would also occur after nocodazole treatment. Third, they suggest that effective cortical actin disruption by latrunculin B requires intact microtubules. Loss of sensitivity to latrunculin B is specific for cortical actin and not displayed by stress fibers. This suggests a function of microtubules in dynamic turnover of cortical actin.

The studies performed with the endocytosis inhibitor tyrphostin A23 have the following implications. First, they once more show that intracellular accumulation of Mrp1 (Abcc1) is due to endocytosis. Second, with this tool, we were able to disconnect the effects of latrunculin B on Mrp1 (Abcc1) internalization from its effects on lipid raft association and efflux activity.

Downloaded from molpharm.aspetjournals.org by guest on December 1, 2012

aspet

In conclusion, cortical actin stabilizes Mrp1/MRP1 (Abcc1/ABCC1) in a lipid raft environment on the cell surface and supports optimal activity of this transporter as an efflux pump. We suggest that loss of the proper lipid raft environment in the context of cortical actin results in loss of Mrp1/MRP1 (Abcc1/ABCC1) activity. Internalization of Mrp1 (Abcc1) does not seem to contribute to the reduced activity but could be a mechanism to remove inactive Mrp1 (Abcc1) molecules from the cell surface. This also implies that it is not the number of ABC transporter molecules on the cell surface that determines overall efflux activity but rather the activity status of cell surface-resident Mrp1/MRP1 (Abcc1/ABCC1) molecules. This activity status in turn depends on properties of the specific membrane domain environment, including the presence of intact cortical actin.

Acknowledgments

We gratefully acknowledge Annie van Dam and Hjalmar Permentier (Mass Spectometry Core Facility, University of Groningen, Groningen, The Netherlands) for their help in the analysis of sphingolipids by liquid chromatography-electrospray ionization tandem mass spectrometry.

Authorship Contributions

Participated in research design: Hummel and Kok.
Conducted experiments: Hummel, Klappe, Ercan, and Kok.
Performed data analysis: Hummel, Klappe, Ercan, and Kok.
Wrote or contributed to the writing of the manuscript: Hummel and Kok.

References

Ananthakrishnan R, Guck J, Wottawah F, Schinkinger S, Lincoln B, Romeyke M, Moon T, and Käs J (2006) Quantifying the contribution of actin networks to the elastic strength of fibroblasts. *J Theor Biol* **242:**502–516.
Bacso Z, Nagy H, Goda K, Bene L, Fenyvesi F, Matkó J, and Szabó G (2004) Raft and cytoskeleton associations of an ABC transporter: P-glycoprotein. *Cytometry A* **61:**105–116.
Bligh EG and Dyer WJ (1959) A rapid method of total lipid extraction and purification. *Can J Biochem Physiol* **37:**911–917.
Brown DA and London E (2000) Structure and function of sphingolipid- and cholesterol-rich membrane rafts. *J Biol Chem* **275:**17221–17224.
Chang XB, Hou YX, and Riordan JR (1997) ATPase activity of purified multidrug resistance-associated protein. *J Biol Chem* **272:**30962–30968.
Chichili GR and Rodgers W (2007) Clustering of membrane raft proteins by the actin cytoskeleton. *J Biol Chem* **282:**36682–36691.
Dudeja PK, Anderson KM, Harris JS, Buckingham L, and Coon JS (1995) Reversal of multidrug resistance phenotype by surfactants: relationship to membrane lipid fluidity. *Arch Biochem Biophys* **319:**309–315.
Gamble W, Vaughan M, Kruth HS, and Avigan J (1978) Procedure for determination of free and total cholesterol in micro- or nanogram amounts suitable for studies with cultured cells. *J Lipid Res* **19:**1068–1070.
Hinrichs JW, Klappe K, Hummel I, and Kok JW (2004) ATP-binding cassette transporters are enriched in non-caveolar detergent-insoluble glycosphingolipid-enriched membrane domains (DIGs) in human multidrug-resistant cancer cells. *J Biol Chem* **279:**5734–5738.
Kikuchi S, Hata M, Fukumoto K, Yamane Y, Matsui T, Tamura A, Yonemura S, Yamagishi H, Keppler D, Tsukita S, et al. (2002) Radixin deficiency causes conjugated hyperbilirubinemia with loss of Mrp2 from bile canalicular membranes. *Nat Genet* **31:**320–325.
Lavie Y, Fiucci G, and Liscovitch M (1998) Up-regulation of caveolae and caveolar constituents in multidrug-resistant cancer cells. *J Biol Chem* **273:**32380–32383.
Luciani F, Molinari A, Lozupone F, Calcabrini A, Lugini L, Stringaro A, Puddu P, Arancia G, Cianfriglia M, and Fais S (2002) P-glycoprotein-actin association through ERM family proteins: a role in P-glycoprotein function in human cells of lymphoid origin. *Blood* **99:**641–648.
Macdonald JL and Pike LJ (2005) A simplified method for the preparation of detergent-free lipid rafts. *J Lipid Res* **46:**1061–1067.
Mundy DI, Machleidt T, Ying YS, Anderson RG, and Bloom GS (2002) Dual control of caveolar membrane traffic by microtubules and the actin cytoskeleton. *J Cell Sci* **115:**4327–4339.
Radeva G, Perabo J, and Sharom FJ (2005) P-Glycoprotein is localized in intermediate-density membrane microdomains distinct from classical lipid rafts and caveolar domains. *FEBS J* **272:**4924–4937.
Romsicki Y and Sharom FJ (1999) The membrane lipid environment modulates drug interactions with the P-glycoprotein multidrug transporter. *Biochemistry* **38:**6887–6896.
Schroeder R, London E, and Brown D (1994) Interactions between saturated acyl chains confer detergent resistance on lipids and glycosylphosphatidylinositol (GPI)-anchored proteins: GPI-anchored proteins in liposomes and cells show similar behavior. *Proc Natl Acad Sci USA* **91:**12130–12134.
Sinicrope FA, Dudeja PK, Bissonnette BM, Safa AR, and Brasitus TA (1992) Modulation of P-glycoprotein-mediated drug transport by alterations in lipid fluidity of rat liver canalicular membrane vesicles. *J Biol Chem* **267:**24995–25002.
Smith PK, Krohn RI, Hermanson GT, Mallia AK, Gartner FH, Provenzano MD, Fujimoto EK, Goeke NM, Olson BJ, and Klenk DC (1985) Measurement of protein using bicinchoninic acid. *Anal Biochem* **150:**76–85.
Spector I, Braet F, Shochet NR, and Bubb MR (1999) New anti-actin drugs in the study of the organization and function of the actin cytoskeleton. *Microsc Res Tech* **47:**18–37.
Sullards MC and Merrill AH Jr (2001) Analysis of sphingosine 1-phosphate, ceramides, and other bioactive sphingolipids by high-performance liquid chromatography-tandem mass spectrometry. *Sci STKE* **2001:**PL1.
Sullards MC, Wang E, Peng Q, and Merrill AH, Jr. (2003) Metabolomic profiling of sphingolipids in human glioma cell lines by liquid chromatography tandem mass spectrometry. *Cell Mol Biol* **49**:789–797.

Address correspondence to: Dr. Jan Willem Kok, University Medical Center Groningen, University of Groningen, Department of Cell Biology, Section Membrane Cell Biology, A. Deusinglaan 1, 9713 AV Groningen, The Netherlands. E-mail: j.w.kok@med.umcg.nl

MOL PHARM
MOLECULAR PHARMACOLOGY
aspet
Downloaded from molpharm.aspetjournals.org by guest on December 1, 2012